A High Resolution Lunar Gravity Field and Predicted Orbit Behavior

A. S. Konopliv
W. L. Sjogren
R. N. Wimberly
R. A. Cook
V. Alwar

Jet Propulsion Laboratory
California Institute of Technology
4800 Oak Grove Drive
Pasadena, California91109

ABSTRACT

A spherical harmonic lunar gravity field of degree and order 60 has been developed using two-way and three-way Doppler data from the Lunar Orbiter I, II, III, IV, and V missions. The Lunar Orbiter missions provided data in 1967 ant] 1968 in high inclination orbits (IV and V) and in near equatorial orbits (1, II, and 111), This data set provides global gravity coverage directly for the nearside and indirectly for the farside. The gravity field will be evaluated by comparing resolution of surface features with previous existing gravity fields such as the field determined by Bills and Ferrari [1980] and also by prediction of the Apollo 16 subsatellite crash. implications on navigation of a lunar orbiter will also be discussed. Propagation of satellite position error due to the 60th degree and order lunar gravity field covariance for different lunar orbits will be presented as well as behavior of lunar circular orbits, existence of frozen orbits, anti fuel costs for orbit maintainance.

Method

The gravity field is determined by merging the gravit y information from 64 arcs of data from LO I, 82 arcs of data from 1..011, 66 arcs of data from 1.0111, 14 arcs of data from 1.0 IV, ant] 60 arcs of data from LO V. This data set encompasses al] the tracking data for the Lunar Orbiter missions except four clays of 1.0 I data that we were unable to recover from magnetic tape and the high altitude data for LO IV which contains minima] gravity information. The arcs are at most one day long (at most eight orbits) anti for each arc the spacecraft state, solar pressure coefficients, maneuver delta velocities, and three-way Doppler biases are estimated. The global parameters that are common to all data arcs are the DSN station locations, GM of the Moon, ant] the 60th degree and order gravity field for a total of 37 1'/ global parameters. The global parameters are determined by merging the information matrices of the global parameters from all the data arcs in squareroot information (SRIF) form and by applying a constraining a priori covariance based upon Kaula's [1966] stress rule.

Results

The radial accelerations at 100 km above the mean surface of the 60th degree anti order gravity model arc displayed in Figure 1. This demonstrates the high correlation of the gravity field with surface feat ures especiall y on the nearside and that general features are

The Properties of CrN/Au and Cr/CrN/Au Multilayers,

E. Kolawa[1], **D.** Lie[2], J. Reid[2], B. Tai[1], L. Lowry[1] and J. Scott-Monck[1]1 Jet Propulsion Laboratory, 4800 Oak Grove Dr. , Pasadena (A 91109. [2] California institute of7'ethnology Dept. of Applied Physics 116-81, Pasadena CA 91125.

Gold has been used as a conductor material in many microelectronic applications because of its low resistivity, bondability, and oxidation/ corrosion resistance. However, the adhesion of gold layers deposited on glass, ceramics or oxidized substrates is rather poor and a thin multilayer of some metal such as chromium is used to provide the bond. It is well known that significant interdiffusion between Au and (r takes place at reasonably low temperatures resulting in the rapid increase in the resistance of the gold layer. in this paper we report on the diffusion barrier performance of reactively sputtered CrN layers of different compositions. We have employed backscattering spectrometry, cross sectional transmission electron microscopy, and sheet resistance measurements to characterize the samples processed at different temperatures. The mechanical stress of individual films and the multilayer structures before and after heat treatment was determined using high resolution x-ray diffraction techniques. Modified peel tests were applied to both CrN/Au and Cr/CrN/Au multilayers deposited on silicon oxide and aluminum nitride to test the adhesion of the layers. Our results show that the CrN layer is able to prevent the interdifussion of the Cr and Au up to 200C for a 60 minute heat treatment but the adhesion of the CrN to the silicon oxide substrate is poor. An addition of a thin Cr layer improves the adhesion resulting in a thermally stable and well bonded interconnection scheme.

being resolved on the farside by indirect measurements, i.e. observing the integrated effect of the acceleration on the farside once tracking on the nearside resumes. Figures 2, **3,** 4, and 5 show the improvement in the LO V residuals for the 60th degree and order model over the Bills and Ferrari 16th degree and order model. When periapse is on the nearside, residual amplitudes for one day arcs are reduced by nearly a factor of 100 and when periapse is on the farside, residual amplitudes are reduced by nearly a factor of 1000. The Apollo 16 subsatellite crash which occurred 35 days after release is predicted by our model within a day (i.e. within the errors due to the uncertainty in the initial conditions). Also circular orbit behavior is closer to the smooth end of the spectrum that different gravity fields predict, The Liu-Laing [1971] model predicts a 100-km circular orbit will crash in less than 40 days and the periapse altitude for our model is at about 50 km after 100 days.

Acknowledgements

This work was carried out by the Jet Propulsion Laboratory, California institute of Technology, under contract with the National Aeronautics and Space Administration.

References

Bills, B. G. and A. J. Ferrari, "A Harmonic Analysis of Lunar Gravity," Journal of Geophysical Research, Vol. 8S, No. B, pp. 1013-1025, 1980.

Kaula, W. M., Theory of Satellite Geodesy, Blaisdell Publishing Company, Waltham, Massachusetts, 1966.

Liu, A, S. and P. S. L.sing, "Lunar Gravity Analysis from Long Term Effects," Science, Vol. 173, pp. 1017-1020, 1971.

Figure 1: Free air acceleration at 100 km altitude for 60x60 gravity field.

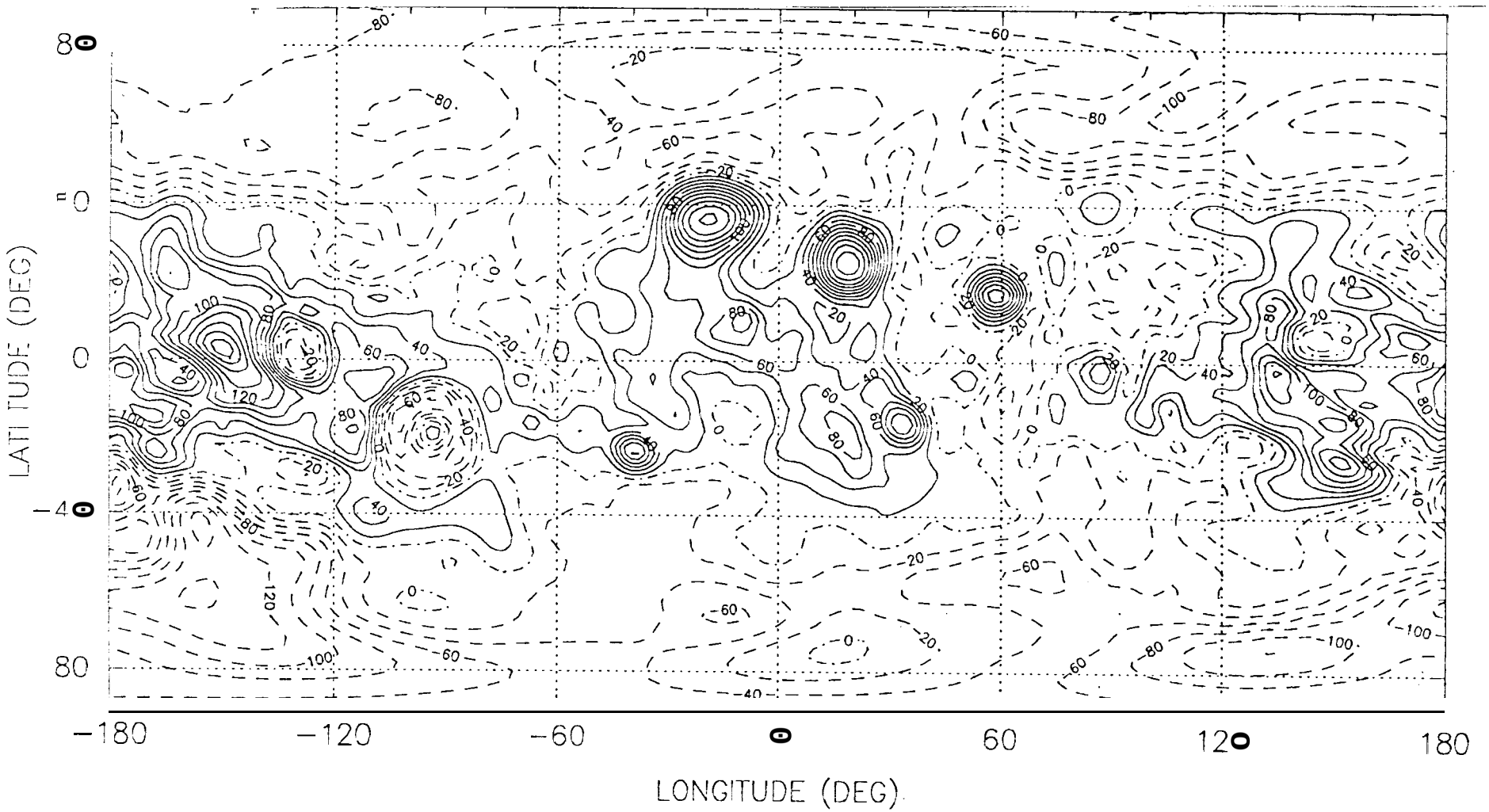

Fig. 2: Sample LO V Nearside Residuals for ~~Lunbag~~ 60x. 60

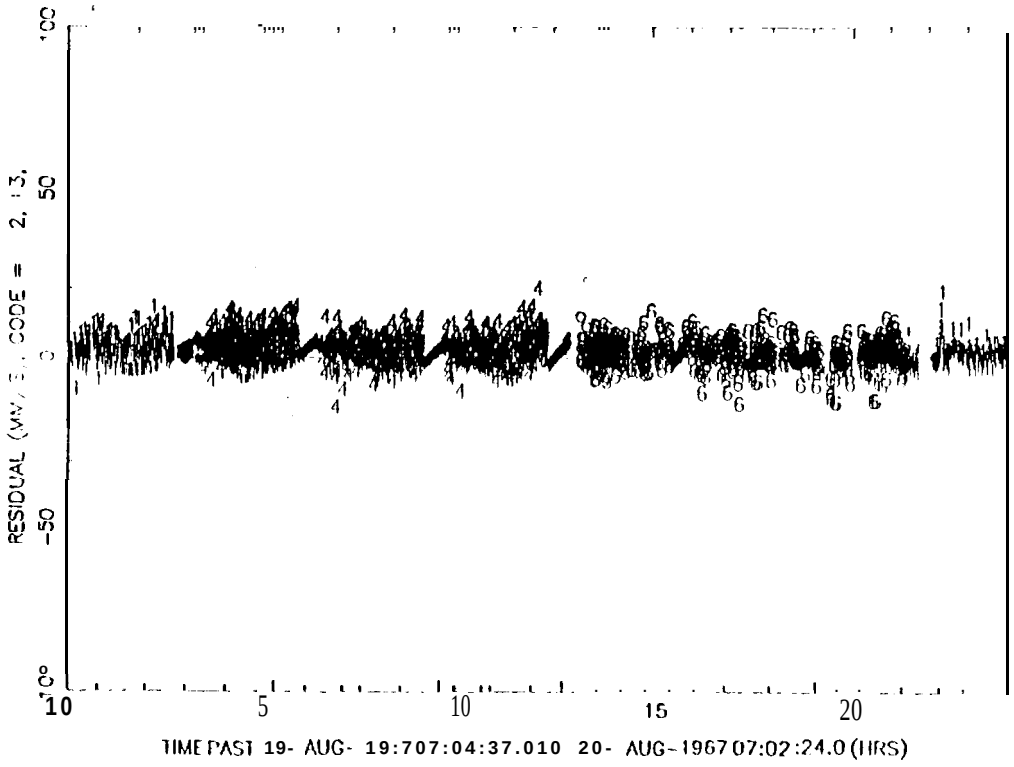

17

Fig 3: Sample 10 V Nearside Residuals for Bills - Ferrari

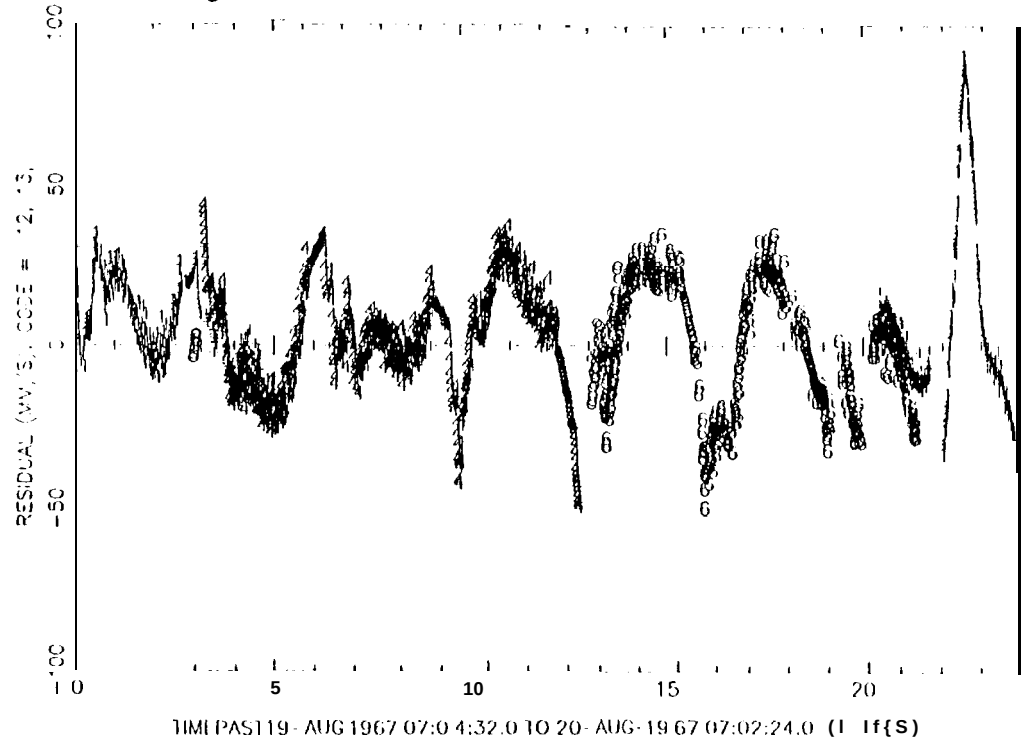

2B

Fig 4: Sample LO V Farside Residuals for Lun50g

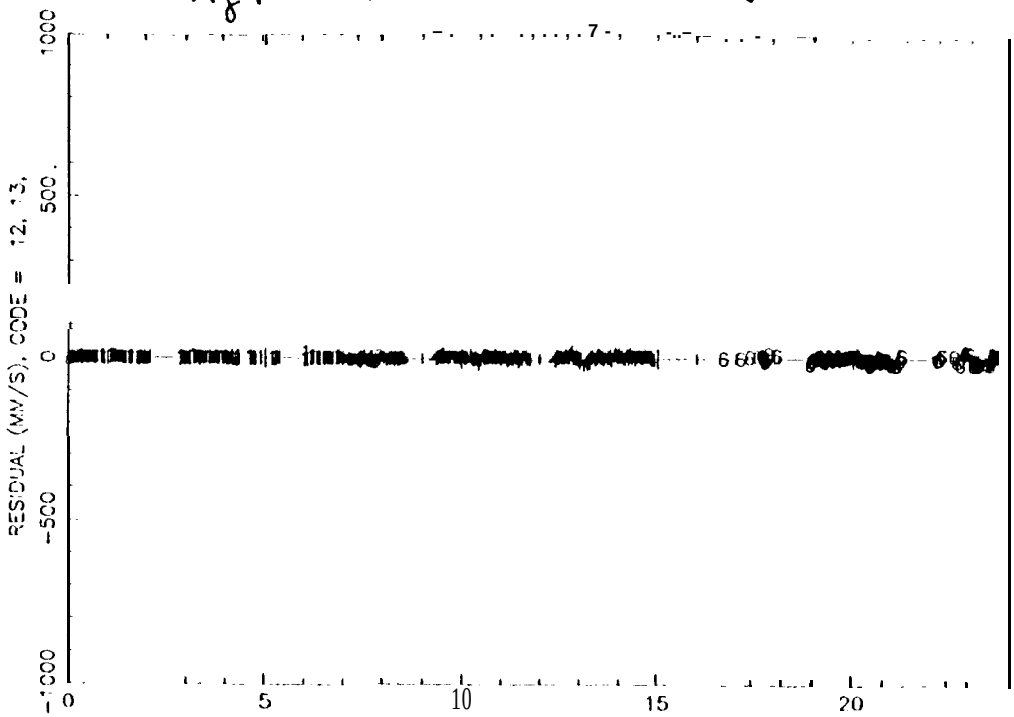

Fig 5: Sample LO V Farside Residuals for Bills-Ferrari